UNIVERSIDAD DISTRITAL
FRANCISCO JOSÉ DE CALDAS

Visión Electrónica

https://revistas.udistrital.edu.co/index.php/visele

VISIÓN ELECTRÓNICA

A CASE-STUDY VISION

Electromagnetic system based on Long Range Wireless Technology (LoRa) for monitoring the Chiles – Cerro Negro Volcanic Complex

Sistema Electromagnético basado en Tecnología Inalámbrica de Largo Alcance (LoRa) para Monitoreo del Complejo Volcánico Chiles – Cerro Negro

Wilson Leonel Enríquez López [1], Karen Elizabeth Loaiza Jiménez [2], Christian Jonathan Espín Ibarra [3], María Cristina Ramos López [4], Daniel Felipe Cárdenas López [5]

INFORMACIÓN DEL ARTÍCULO

Historia del artículo:
Enviado: 06/10/2024
Recibido: 25/10/2024
Aceptado: 10/12/2024

Keywords:
Electromagnetic Fields
LoRa - TDMA
Magnetometric Sensors
Volcanic Monitoring
Wireless Transmission

Palabras clave:
Campos Electromagnéticos
LoRa - TDMA
Monitoreo Volcánico
Sensores Magneto Métricos
Transmisión Inalámbrica

ABSTRACT

A system has been designed for monitoring the environment of the Chiles – Cerro Negro volcanic complex in Ecuador, composed of electromagnetic field sensors and long-distance wireless transmission technology with low energy consumption called LoRa (Long Range). Additionally, a time division multiple access (TDMA) communication method has been used, which helps reduce the probability of collision and improve the reliability of data transmission of a standard LoRa network. First, system tests were carried out by quickly uploading data to the terminal located from 500 meters to 3 kilometers from the Gateway LG01-P, observing that the packet loss rate was reduced by 11%. These tests motivated the installation of the system at a point closer to the volcano, choosing the "Chiles2" station as a reference at the coordinates 0.802470 latitude and -77.917900 longitude. The data is collected in a .csv file and sent from the "Chiles2" station to the Tulcán Prefecture. Since there are 15 kilometers between these two points, Yagi antennas were placed to enhance the LoRa wireless transmission and ensure communication with the LG01-P Gateway. The .csv files are read with a program developed in LabVIEW and the signal is processed with a moving average filter of order 7. This has allowed obtaining a filtered and clean signal that will be used for later analysis and information processing. Likewise, these results show that the magnetometric sensors acquire measurements within the expected range and that LoRa wireless technology can be used for signal transmission.

1 Electronics and Telecommunications Engineering, Escuela Politécnica Nacional, Ecuador. Communications Engineering, Universidad de Cantabria, España. Ph. D (c) in Electrical Engineering, Universidad Federal de Santa Catarina, Brasil. Current position: Main Professor Escuela Politécnica Nacional / Instituto Geofísico, Ecuador. E-mail: wenriquez@igepn.edu.ec

2 Electronics and Telecommunications Engineering, Escuela Politécnica Nacional, Ecuador. Master's degree in Telecommunication Networks and Services, Universidad de Buenos Aires, Argentina. Current position: Instrumentation Network Specialist / Escuela Politécnica Nacional / Instituto Geofísico, Ecuador. E-mail: kloaiza@igepn.edu.ec

3 Electronics and Telecommunications Engineering, Escuela Politécnica Nacional, Ecuador. Instrumentation Network Analyst / Escuela Politécnica Nacional / Instituto Geofísico, Ecuador. E-mail: cespin@igepn.edu.ec

4 Electronics and Telecommunications Engineering, Escuela Politécnica Nacional, Ecuador. Master's degree in Wireless Systems and Related Technologies, Politécnico di Torino, Italia. Current position: Full Professor Escuela Politécnica Nacional / Instituto Geofísico, Ecuador. E-mail: cramos@igepn.edu.ec

5 Electronics and Telecommunications Engineering, Escuela Politécnica Nacional, Ecuador. Master's degree in Optical Communication and Photonic Technologies, Politécnico di Torino, Italia. Current position: Principal Investigator / University College London, UK. E-mail: danielsj18@yahoo.com

Citar este artículo como: W. L. Enríquez López, K. E. Loaiza Jiménez, C. J. Espín Ibarra, M. C. Ramos López, D. F. Cárdenas López, "Electromagnetic system based on Long Range Wireless Technology (LoRa) for monitoring the Chiles – Cerro Negro Volcanic Complex", Visión electrónica, vol. 18, no. 2, pp. 298-308, july-december 2024, https://doi.org/10.14483/22484728.23629

Finally, from the measurements obtained in the geothermal area of the Chiles volcano, different anomalies in the magnetic field could be observed, especially when high seismic events or activities occur. In this sense, the data obtained in this project will be analyzed in conjunction with other monitoring parameters, such as seismic activity, etc., and a more complete image of the activity of the volcanic complex under study will be obtained. Finally, this document presents the final results that have allowed the Geophysical Institute of the National Polytechnic School to obtain the measurement of the magnetic fields produced during the seismic activity of the Chiles – Cerro Negro volcanic complex in the period October 2022.

RESUMEN

Se ha diseñado un sistema para monitoreo del entorno del complejo volcánico Chiles – Cerro Negro en Ecuador compuesto por sensores de campo electromagnético y tecnología de transmisión inalámbrica de larga distancia con bajo consumo de energía denominada LoRa (Long Range). Adicionalmente se ha utilizado un método de comunicación de acceso múltiple por división de tiempo (TDMA) que ayuda a reducir la probabilidad de colisión y mejorar la confiabilidad de la transmisión de datos de una red LoRa estándar. Primero se realizaron pruebas del sistema mediante la carga rápida de datos al terminal ubicado desde 500 metros hasta 3 kilómetros de la puerta de enlace Gateway LG01-P observando que la tasa de pérdida de paquetes se reduce en un 11%. Estas pruebas motivaron a instalar el sistema en un punto más cercano al volcán, eligiendo referencia la estación “Chiles2” en las coordenadas 0,802470 de latitud y -77.917900 de longitud. Los datos son recopilados en un archivo tipo .csv y enviados desde la estación “Chiles2” hasta la Prefectura de Tulcán. Debido que entre estos dos puntos existen 15 kilómetros de distancia, se colocaron antenas Yagi para potenciar la transmisión inalámbrica LoRa y garantizar la comunicación con el Gateway LG01-P. Los archivos .csv se leen con un programa desarrollado en LabVIEW y la señal es procesada con un filtro de promedios móviles (moving average) de orden 7. Esto ha permitido obtener una señal filtrada y limpia que servirá para un posterior análisis y tratamiento de información. Así mismo, estos resultados evidencian que los sensores magneto métricos adquieren mediciones dentro del rango previsto y que se puede utilizar tecnología inalámbrica LoRa para la transmisión de señales.

Finalmente, de las mediciones obtenidas en la zona geotérmica del volcán Chiles se pudo observar distintas anomalías en el campo magnético, especialmente cuando se producen eventos o actividades sísmicas elevadas. En ese sentido, los datos obtenidos en este proyecto serán analizados en conjunto con otros parámetros de monitoreo, como la actividad sísmica, etc. y obtener una imagen más completa de la actividad del complejo volcánico en estudio. Por último, en este documento se presentan los resultados finales que han permitido al Instituto Geofísico de la Escuela Politécnica Nacional obtener la medición de los campos magnéticos producidos durante la actividad sísmica del complejo volcánico Chiles – Cerro Negro en el periodo octubre de 2022.

1. Introduction

The interaction of physical-chemical processes contributes to charges in volcanic activity. Short-term forecasting requires data collection to understand these dynamic processes. Advances in sensor technology, digitizers, telemetry and monitoring records have enabled the observation and quantification of short-term changes, these advancements facilitate data collection stored centrally in near real-time [1].

Electromagnetic phenomena are one method for detecting precursor signals of volcanic eruptions, an area of interest in countries like Japa, USA, and Italy [2]. However, it remains unclear whether electromagnetic signals consistently precede eruptions or correlate with other geophysical signals, such as ground tilt changes or gas emissions, despite evidence linking magnetic field changes to eruptions [2] [3].

Magmatic intrusions cause thermal demagnetization, changes in ground resistivity, and variations in the electric field. Rock factures, fluid and gas movements, stress redistribution and changes in volcanic material properties further disturb the electromagnetic field. Monitoring these disturbances can indicate magmatic intrusions or gas ascensions affecting the volcano’s interior [4].

In this study, the Instituto Geofísico developed a system with electromagnetic field sensors and LoRa wireless technology to monitor the Chiles – Cerro Negro volcanic complex in northern Ecuador. This research highlights the importance of monitoring magnetic fields associated with volcanic activity to better understand the processes of this complex.

2. LoRa Wireless communication technology

LoRa technology has gained acceptance for long-distance communication, particularly in remote or hard-to-reach areas where internet connectivity is limited. It is ideal for deploying networks for monitoring, configuring and controlling sensors in such areas. Table 1 compares LoRa with other Wireless communication technologies.

Table 1. Comparison of LoRa and other Wireless technologies

Type	ZigBee	Wi-Fi	GPRS	LoRa
Access mode	ZigBee Gateway	Wireless Router	Cellular Network	LoRa Gateway
Frequency band	2.4G Hz	2.4G o 5G Hz	900 – 1800M Hz	433 – 915 MHz
Transmission range	10 – 50m	100m	Long range	(1 – 20 km)
Data rate	100kbps	300Mbps	20 – 30kbps	0.3 – 50 kbps
Battery life	2 years	Several hours	Several days	5 years

Source: own.

The main feature of LoRa is CSS (Chirp Spread Spectrum) modulation, which retains the low power consumption of FSK (Frequency Shift Keying) modulation while significantly increasing the communication range. This modulation represents each payload bit of information using multiple chirps, which are defined as a linear frequency sweep over the symbol period. The rate at which are defined as a linear frequency sweep over the symbol period. The rate at which spread information is transmitted is known as the symbol rate. The relationship between the nominal symbol rate and the chirp rate is referred to as the Spreading Factor (SF). This SF determines the chirp rate and, consequently, the transmission speed. In other words, it represents the number of symbols sent per bit of information [5].

When employing CSS modulation, the data rate can be traded for sensitivity using a fixed bandwidth by selecting an SF value between 6 and 12. A low SF means more chirps are sent per second, allowing more data to be encoded per second, resulting in higher transmission rates. Conversely, a higher SF decreases the transmission rate. SF values are orthogonal, meaning that two signals modulated with different spreading factors can coexist at the same frequency and time without interfering with each other. LoRa's range can reach up to 5 kilometers in urban areas and over 15 kilometers in rural regions. Theoretically, it operates on unlicensed frequency bands at 433 MHz, 868 MHz, or 915 MHz (Industrial, Scientific, and Medical—ISM bands) and supports bit rates between 0.37 kbps and 46.9 kbps, offering promising coverage distances over several kilometers [6].

The Coding Rate (CR) in the header refers to the ratio of non-redundant information in the data stream. This parameter can be selected from values of 4/5, 4/6, 4/7, and 4/8. For instance, a 4/6 coding rate indicates that out of 6 total bits, 4 are useful and the rest are redundant. A lower coding rate increases the time a packet remains in the air and lengthens transmission time. This makes data reception easier because the packet spends more time in the air, allowing the receiver to demodulate the information with lower power, thereby improving sensitivity. On the other hand, this impacts power consumption and battery life. If the SNR (Signal-to-Noise Ratio) is greater than 0, the received signal is above the noise floor. Conversely, if the SNR is below 0, the signal is under the noise floor. The RSSI (Received Signal Strength Indicator) represents the received radio signal strength, measured in dBm as a negative value. The closer this value is to 0, the stronger or better the received signal [5].

The LoRa packet structure is in Figure 1. The section between the preamble and payload is encoded at a fixed coding rate, for instance, 4/8, while the payload coding rate and CRC are optional within a

specific range. As a result, the encoded payload length and its CRC are variable, depending on the selected coding rate [7].

Figure 1. LoRa packet structure

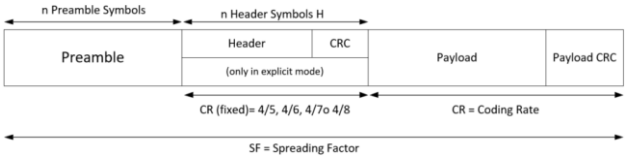

Source: own.

A LoRa network consists of end devices and a gateway. End devices are sensors that wirelessly connect to the gateway. The gateway receives messages from any sensor within its coverage range and forwards these messages to the server designated by the end client. Gateway traffic can be transmitted to a server via Wi-Fi, Ethernet, or other means. It is essential to note that the LoRa gateway operates solely at the physical layer and only verifies the integrity of the received data. If the Cyclic Redundancy Check (CRC) is incorrect, the message will be discarded. Conversely, if the CRC is correct, the gateway forwards the message to the server, along with additional information such as the Received Signal Strength Indicator (RSSI) level. Additionally, when using Time Division Multiple Access (TDMA), synchronization is required among the devices within the LoRa network to ensure seamless communication [5].

3. Development of the magneto metric system model

The magnetic field model for two stations, developed by the Instituto Geofísico, is based on solving Maxwell's equations for two points under boundary conditions for partially conductive mediums, as shown below:

$$\nabla xH = (\sigma + j\omega\varepsilon)E = J + \frac{\partial D}{\partial t} \qquad (1)$$

$$\nabla xE = -j\omega\mu H = -\frac{dB}{dt} \qquad (2)$$

$$\nabla . E = \rho \qquad (3)$$

$$\nabla . H = 0 \qquad (4)$$

Donde:

$$H = \ Magnetic\ Field$$

$$E = \ Electric\ Field$$

$$\sigma = Electrical\ Conductivity$$

$$\varepsilon = Electrical\ Permittivity$$

$$\mu = Magnetic\ Permeability$$

The wave solution is obtained by applying the Vector Identity:

$$\nabla x(\nabla xA) = \nabla(\nabla . A) - \nabla^2 A$$

$$\nabla^2 A = (\nabla^2 A_x)a_x + (\nabla^2 A_y)a_y + (\nabla^2 A_z)a_z$$

Using equations (1) and (2) and applying equations (3) and (4):

$$-\nabla^2 H = (\sigma + j\omega)(\nabla xE)$$

$$-\nabla^2 E = (-j\omega\mu)(\nabla xH)$$

Now, using $(\nabla xE) and\ (\nabla xH)$, the wave equation is derived.

$$\nabla^2 H = \gamma^2 H \ ^\wedge \ \nabla^2 E = \gamma^2 E$$

Where:

$$\gamma^2 = j\omega\mu(\sigma + j\omega\varepsilon)$$

And

$$\gamma = \alpha + jB$$

$$\alpha = \omega \sqrt{\frac{\mu\varepsilon}{2}\left(\sqrt{1+\left(\frac{\sigma}{\omega\varepsilon}\right)^2}\right)-1} \qquad (5)$$

$$\beta = \omega \sqrt{\frac{\mu\epsilon}{2}\left(\sqrt{1+\left(\frac{\sigma}{\omega\epsilon}\right)^2}\right)+1} \qquad (6)$$

The constant α is referred to as the attenuation factor, and β is known as the phase shift constant. For a region with moderate conductivity, such as wet soil, rocky terrain, or clay, which characterizes volcanic lands, the solution for E is as follows:

$$E = E_o e^{-\gamma z} a_x$$

Thus, from equation (2):

$$H = \sqrt{\frac{\sigma + j\omega\varepsilon}{j\omega\mu}}\, E_o\, e^{-\gamma z} a_z$$

The ratio E/H characterizes the medium more specifically: $E = E_x a_x$ propagating in z.

$$H = H_y a_y$$

The intrinsic impedance η of the medium is defined as:

$$\eta = \frac{E_x}{H_y}$$

$$\eta = \sqrt{\frac{j\omega\mu}{\gamma + j\omega\varepsilon}}$$

Where, $\eta = |\eta| \angle\theta$ with

$$|\eta| = \frac{\sqrt{\frac{\mu}{\varepsilon}}}{\sqrt[4]{1+\left(\frac{\sigma}{\omega^2}\right)^2}}$$

$$\tan(2\theta) = \frac{\sigma}{\omega\varepsilon} \quad \text{y} \quad 0° < \theta \leq 45°$$

If the wave propagates in $-Z \Rightarrow Ex/Hy = \eta$. γ it is substituted $-\eta$ and the other square root is used.

By introducing the time factor $e^{+j\omega t}$ and by wiring $\gamma = \alpha + jB$, the following equations for the electromagnetic field are obtained.

$$E(z,t) = E_o e^{-\alpha z} e^{j(\omega t - Bz)} a_x$$

$$H(z,t) = \frac{E_o}{|\eta|} e^{-\alpha z} e^{j(\omega t - Bz - a_x)} a_y$$

The factor $e^{-\alpha z}$ attenuates the magnitudes E *and* H in the $+Z$ *direction.* Similarly, the phase difference θ vanishes in $E(z,t)$ *and* $H(z,t)$ when $\sigma = 0$.

The propagation velocity and wavelength are given by:

$$\upsilon = \frac{\omega}{\beta} = 1/\sqrt{\frac{\mu\varepsilon}{2}\left(\sqrt{1+\left(\frac{\sigma}{\omega\varepsilon}\right)^2}+1\right)}$$

$$\lambda = \frac{2\pi}{\beta} = 2\pi/\sqrt{\frac{\omega\varepsilon}{2}\left(\sqrt{1+\left(\frac{\sigma}{\omega\varepsilon}\right)^2}+1\right)}$$

It is known that $\lambda f = \upsilon$, which can be used to calculate the wavelength.

The term $\left(\frac{\sigma}{\omega\varepsilon}\right)^2$ reduces both the velocity and the wavelength.

If the material is dielectric $\alpha = 0$

If the material is a good conductor:

$$\upsilon = \sqrt{2\omega/\mu\sigma} = \omega\delta \qquad \lambda = \frac{2\pi}{B} = \frac{2\pi}{\sqrt{\pi f\mu\sigma}} = 2\pi\delta$$

Where $\delta = penetration\ depth$

$$\delta = \frac{1}{\sqrt{\pi f\mu\sigma}} = \frac{1}{\alpha}(m)$$

Applied to an x, y plane, we have:

P1: Position of station 1

P2: Position of station 2

Figure 1. x, y Plane: Station Positions

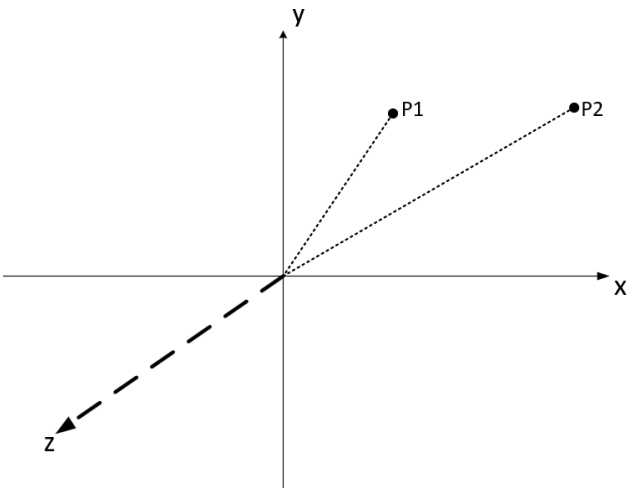

Source: own.

Depending on the type of soil in the Andean volcanoes, the field strength and the internal magma flow exhibit variations. In Ecuador, the electromagnetic field is expected to range between $28000\ y\ 30000\ nT$. The fields will vary according to the distance (z) from the sensor to the flow. Thus, the calculated fields are:

$$E1 = E_{o1}sen(\omega t + Bz)a_x + E_{o1}cos(\omega t + Bz)a_y \quad (7)$$

$$H1 = H_{o1}cos(\omega t + Bz)a_x + E_{o1}cos(\omega t + Bz)a_y \quad (8)$$

$$E2 = E_{o2}sen(\omega t + Bz)a_x + E_{o2}cos(\omega t + Bz)a_y \quad (9)$$

$$H2 = H_{o2}cos(\omega t + Bz)a_x + H_{o2}sen(\omega t + Bz)a_y \quad (10)$$

Where:

Point1: $E1$ and $H1$

Point2: $E2$ and $H2$

ω: Measurement frequency at low frequency.

E_{01}, H_{01}, B: Site-specific constants that depend on the properties of the soil materials.

4. System description

4.1 Equipment

Transmitter node:

High-precision scalar magnetometer GSM-90 v7.0: The main device for the Project.

- GPS Module for Arduino UNO.
- LoRa Radio Transmitter Module: Enables long-range communication.
- Autonomous Power System: Includes solar panels, a voltaje regulator and batteries to extend system autonomy, particularly due to the power consumption of the magnetometer.
- Arduino UNO-based controller: Manages all connected devices and implements three serial communication interfaces:

Two UARTs: One communicates with the magnetometer, and the other with the GPS receiver and computer for monitoring purposes.

One SPI interface: Used for communication with the LoRa radio transmitter module.

Receptor node:

- LG01-P Gateway: A commercial platform from Dragino based on Arduino. This device features:

AR9331 Board: Equipped with a MIPS 24K processor running Linux, 16 MB of flash memory, and 64 MB of RAM.

LoRa Technology Module: Functions as a radio receiver.

4.2 Description of the Functioning of the Installed System

The magnetometric system is located at a geothermal source approximately 3 kilometers from the crater of the Chiles volcano. The system is aligned with the existing seismic station named “Chiles 2”, located at latitude 0,802470 and longitude −77.917900, under the ownership of the Instituto Geofísico.

Given its location, the system utilizes LoRa wireless communication with a point-to-multipoint topology, enabling long-range transmission with very low power consumption. The advantage of this technology lies in its low energy requirements, making it ideal for remote scenarios where sensors need to transmit data over extended periods. Consequently, LoRa devices do not require dedicated solar panels or other energy sources that might complicate the hardware setup for operating remote sensors.

To transmit magnetic field data recorded near the Chiles – Cerro Negro volcanic complex, Arduini Shield modules were chosen for their ease of integration with the LoRa chip via programming on an Arduino UNO-based controller. Additionally, the Dragino commercial platform, designed for the Internet of Things (IoT), was selected. This platform leverages Arduino technology and Linux-based microprocessor system to act as a gateway, complementing the sensor network.

To transmit magnetic field data recorded near the Chiles – Cerro Negro volcanic complex, Arduino Shield modules were chosen for their ease of integration with the LoRa chip via programming on an Arduino UNO-based controller. Additionally, the Dragino commercial platform, designed for the Internet of Things (IoT), was selected. This platform leverages Arduino technology and a Linux-based microprocessor system to act as a gateway, complementing the sensor network.

The installation of seismic monitoring equipment enables the observation and quantification of short-term changes in the volcano. In this case, the use of magnetometric sensors provides an additional tool for the Instituto Geofísico's monitoring network and serves to measure magnetic fields in volcanic regions. Specifically, the magnetometric sensor at the “Chiles 2” seismic station collects magnetic field values from the Chiles – Cerro Negro volcanic complex and transmits them using LoRa wireless technology to the LG01-P Gateway, located at the Tulcán Prefecture.

The LG01-P Gateway is responsible for locally loading the data into a spreadsheet that updates with each reading. The stored data file is remotely accessible due to the gateway's Ethernet connectivity. The gateway acts as the final receiving node and functions as the master controller, polling data from each transmitting station at any given time. Regarding power supply, no additional energy sources were required because the gateway is installed at the same site as the repeater station of the Tulcán Prefecture, which is part of the national monitoring network.

The system structure diagram is illustrated in Figure 2.

5. Time Division Multiple Access (TDMA) Application

The proposed system is designed for automatic connection and random access, leveraging LoRa’s operational characteristics and Time Division Multiple Access (TDMA) communication. This setup reduces data load collisions from transmitting nodes and improves the channel utilization rate towards the gateway. Additionally, it keeps data updated, especially when environmental conditions in the volcanic complex change or fluctuate.

Figure 2. System Architecture

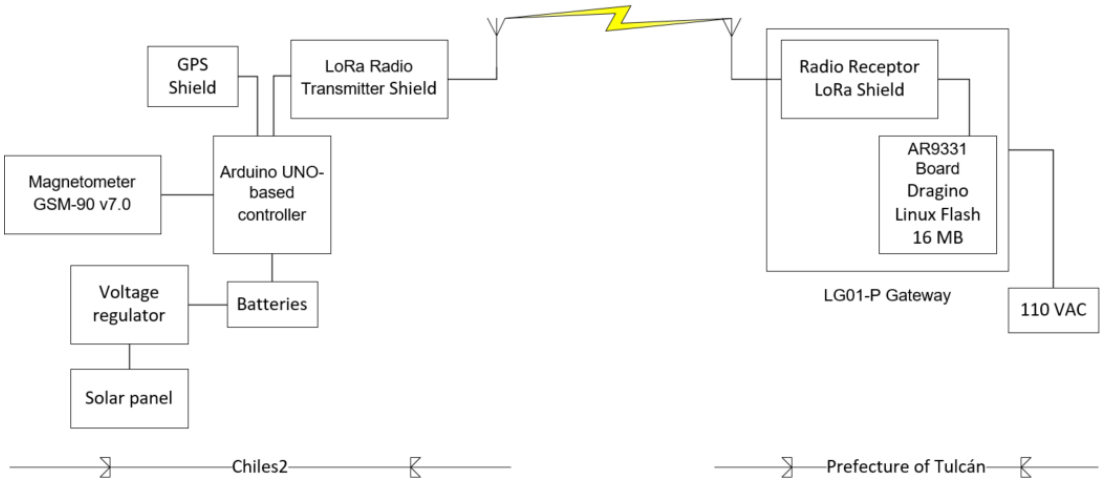

Source: own.

TDMA multiplexing is a technology that uses discrete time pulses to form non-overlapping multiplexes, commonly used in digital communication. Since the channel's bit transmission rate exceeds each channel's data transmission rate, it can be divided into several time segments to be used by multiple signals alternately. Each time segment is separately occupied by a multiplexed signal, allowing for the transmission of multiple digital signals within a physical channel over a specified period. The TDMA strategy divides communication time into small time slots for each terminal to communicate. It is necessary to calculate the maximum air transmission time required for LoRa to load a data packet, which includes a preamble and payload data [8].

The air transmission time of a data packet can be obtained using the following equation (11):

$$T_{packet} = T_{preamble} + T_{payload} \qquad (11)$$

Where $T_{preamble}$ is the transmission time of the preamble and $T_{payload}$ is the transmission time of the payload data.

The preamble transmission time is calculated using equation (12).

$$T_{preamble} = \left(n_{preamble} + 4.25\right) \times T_{sym} \qquad (12)$$

Where $n_{preamble}$ is the length of the preamble and T_{sym} is the symbol time.

The symbol time is calculated using equation (13).

$$T_{sym} = \frac{2^{SF}}{BW} \qquad (13)$$

Where SF is the spreading factor and BW is the bandwidth.

The payload transmission time is calculated using equation (14).

$$T_{payload} = payloadSymbNb \times T_{sym} \qquad (14)$$

Where $payloadSymbNb$ is the number of payload symbols.

The number of payload symbols is calculated using equation (15).

$$payloadSymbNb = 8 + \max\left[ceil\left(\frac{8PL-4SF+28+16CRC-20H}{4(SF-2DE)}\right)(CR+4);\ 0\right] \quad (15)$$

For explicit mode (default), $H = 0$. For implicit mode, $H = 1$. When low data rate optimization is enabled (Adaptive Data Rate) $DE = 1$. Otherwise, $DE = 0$.

CRC enabled means $CRC = 1$, and CRC disabled means $CRC = 0$. For LoRa, the default is $CR = 1$. CR represents the coding rate for the payload and can take values of 1, 2, 3, or 4. For LoRa, the default is $CR = 1$.

From equation (15) it follows that when the SF (Spreading Factor) value is higher, the air transmission time is longer. In this sense, to calculate the maximum required transmission time, the maximum SF should be set to 12, with $BW = 500\,kHz$, $CR = 1$, a payload length PL de 12 bytes, and a preamble of 8 bytes [9].

In our case, the default values of the Dragino kit were used, resulting a preamble transmission time of:

$$T_{preamble} = 12{,}544\,ms$$

The payload transmission time is:

$$T_{payload} = payloadSymbNb \times T_{sym} = 33{,}792\,ms$$

The total air transmission time for a data packet is:

$$\begin{aligned} T_{packet} &= T_{preamble} + T_{payload} \\ &= 12{,}544 + 33{,}792 \\ &= 46{,}336\,ms \end{aligned}$$

The TDMA strategy can efficiently complete data transmission, relying on synchronization between the Gateway clock and the transmitter node clock. The real-time clock (RTC) module in the Gateway controller can retrieve the exact current time at one-hour intervals and synchronize it with the transmitter node's clock. This ensures a reduced probability of data collision [10].

6. Results

Before installing the system in the Chiles–Cerro Negro volcanic complex, functional tests were conducted in a laboratory environment and later at the Guagua Pichincha volcano using LoRa transmission devices. Communication links between the devices and the LG01-P Gateway were established, with a tested range of 500 meters to 3 kilometers, resulting in an 11% reduction in packet loss. These tests were conducted using the omnidirectional antennas included in the Dragino kit and employing the manufacturer's standard transmission parameters for medium range, including: Transmission power of 10 dBm (maximum 23 dBm), banwidth of 125 kHz (maximum 500 kHz), coding rate of 4/5 (maximum 4/8), spreading factor SF of 128 chirps/symbol (maximum 4096 chirps/symbol) equivalent to SF7, and enabled CRC, achieving a data rate of 9,375 kbps.

Following these initial tests, the system was installed at the *"Chiles2"* station in the volcanic complex to collect data from a location closer to the Chiles volcano. The distance between *"Chiles2"* and the Tulcán Prefecture is 15 kilometers in a straight line. To enhance LoRa wireless transmission, Yagi antennas were installed, replacing the omnidirectional antennas from the Dragino kit. With these new antennas, the default transmission parameters were retained, yielding positive results in communication with the LG01-P Gateway at the Tulcán Prefecture.

With the system fully installed, magnetic field data was collected at the *"Chiles2"* station, along with seismic signals from the existing monitoring network in this moderately active volcanic complex. The magnetic field data was saved in .csv files for subsequent signal filtering and analysis. A program developed in LabVIEW was used to process the files, incorporating a 7th-order moving average filter to remove transient readings considered as noise, which fluctuated around ±100 nT relative to the stable measurements

oscillating between 28,800 nT and 28,600 nT, as shown in Figure 3.

Figure 3. Example of the effect of the 7th-order "moving average" filter across the entire signal range of the magnetometric system located at the "*Chiles2*" station.

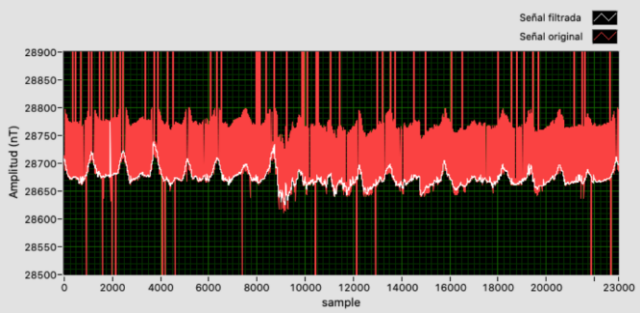

Source: own.

Once the clean signal was obtained, Figure 4 presents the graph of the data recorded by the magnetometer sensor at the *"Chiles2"* station. These satisfactory results demonstrate that the system performs as expected and that the sensors produce measurements within the anticipated range. Although the results are still preliminary, this research highlights the importance of complementing volcano monitoring stations with magnetic field measurements.

Figure 4. Final graph of the signal captured by the sensor located at the "Chiles2" station

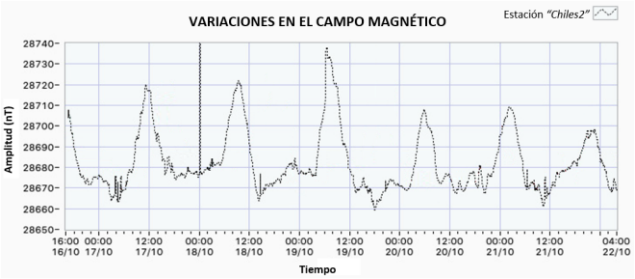

Source: own.

7. Conclusions

The developed magnetometric system aids in the early detection of changes in magnetic fields and, in this case, has enabled the collection of measurement data for the Chiles – Cerro Negro volcanic complex. Preliminary results indicate that these data can reveal magnetic field variations during disturbances or events in the volcanic complex.

This research proposal represents an innovative method and complements the monitoring network of the Geophysical Institute. The collected data will be used alongside other monitoring parameters, such as seismic activity, gas emissions, and ground deformation, to provide a more comprehensive picture of the volcanic complex's activity.

Although a broader network of magnetometers and additional sensors (e.g., for gas and GPS data) would be required, these preliminary results mark the beginning of a future investigation to analyze and compare these data with traditional monitoring methods. The application of the cross-correlation method is one option that could prove useful for quantifying or even determining whether magnetic field variations precede seismic signals. These results will be confirmed and presented in the future by the Instituto Geofísico to help optimize response times in the country's early warning procedures.

References

[1] D. Seidl et al., "The multiparameter station at Galeras Volcano (Colombia): concept and realization," *Journal of Volcanology and Geothermal Research*, vol. 125, n.o 1-2, pp. 1-12, 2003. [Online]. Available: https://doi.org/10.1016/S0377-0273(03)00075-1

[2] J. M, "Review of electric and magnetic fields accompanying seismic and volcanic activity," *U.S. Geological Survey*, vol. 18, n.o 5, pp. 441-475, 1997. [Online]. Available: https://doi.org/10.1023/A:1006500408086

[3] V. Surkov y V. Pilipenko, "Estimate of ULF electromagnetic noise caused by a fluid flow during seismic or volcano activity," *Copernicus Publications,* vol. 2, n.o 10, pp. 6475-6497, 2014. https://doi.org/10.5194/nhessd-2-6475-2014

[4] Y. Sasai et al., "Magnetic and electric field observations during the 2000 activity of Miyake-jima volcano, Central Japan," Earth and Planetary Science Letters, vol. 203, n.o 2, pp. 769-777, 2002. [Online]. Available: https://doi.org/10.1016/S0012-821X(02)00857-9

[5] M. Valenciano, "Implementación de un radioenlace LPWAN con tecnología LoRa", Tesis, Universidad de Valladolid, Valladolid, 2022. [Online]. Available: https://uvadoc.uva.es/bitstream/handle/10324/57458/TFG-G5892.pdf?sequence=1&isAllowed=y

[6] R. Piyare, A. Murphy, M. Magno, y L. Benini, "On-Demand LoRa: Asynchronous TDMA for EnergyEfficient and Low Latency Communication in IoT," *Sensors,* vol. 18, n.o 3718, 2018. [Online]. Available: https://doi.org/10.3390/s18113718

[7] C. Guerrero, "Evaluación de los retardos en redes LoRaWAN multisalto con topología lineal," Tesis, Universidad Politécnica Nacional, Quito Ecuador, 2022.

[8] H. Mahmood Jawad, R. Nordin, S. Kamel Gharghan, A. Mahmood Jawad, y Mahamod Ismail, "Energy-efficient wireless sensor networks for precision agriculture: A review," *Sensors*, vol. 17, n.o 8, p. [Online]. Available: https://doi.org/10.3390/s17081781

[9] R. Muñoz, "Modelado y evaluación de la eficiencia del estándar SCHC para el transporte de paquetes IP sobre LoRaWAN", Tesis Maestría, Universidad de Chile, Santiago de Chile, 2020. [Online]. Available: https://repositorio.uchile.cl/bitstream/handle/2250/177977/Modelado-y-evaluacion-de-la-eficiencia-del-estandar-SCHC-para-el-transporte-de-paquetes-IP.pdf?sequence=1

[10] W. Yong, L. Minzan, y Z. Man, "Remote-control system for greenhouse based on opensource hardware," *IFAC,* vol. 52, n.o 30, pp. 178-183, 2019. [Online]. Available: https://doi.org/10.1016/j.ifacol.2019.12.518